

Kinetics of Co(a^4F , b^4F , a^2F) and Ni(a^3F , a^3D , a^1D) Depletion by O₂, NO, and N₂O

R. Matsui, K. Senba, and K. Honma*

Department of Material Science, Himeji Institute of Technology, Kamigori, Hyogo 678-12, Japan

Received: August 30, 1996; In Final Form: October 22, 1996[⊗]

The kinetics of depletion of the first-row transition-metal atoms Co and Ni upon interactions with O₂, NO, and N₂O were studied in a fast-flow reactor at a He pressure of 0.70 Torr. The depletion rate constants were determined for the first and second excited states of both atoms, Co(b^4F_J , a^2F_J) and Ni(a^3D_J , a^1D_2), as well as their ground states, Co(a^4F_J) and Ni(a^3F_J). For all oxidants, inefficient or no depletion was observed for the ground states of both atoms. Low-lying Ni(a^3D_J) also showed inefficient depletion, though this state has 3d⁹4s¹ configuration. The first and second excited states of Co(b^4F_J , a^2F_J), which have the 3d⁸4s¹ configuration, were depleted very efficiently. The depletion of Ni(a^1D_2), the 3d⁹4s¹ configuration, depended on the oxidants; i.e., O₂ depleted this state by the gas kinetics rate constant, while the depletion by NO and N₂O was about 1 order of magnitude slower. Efficient depletion of the atoms of 3d^{*n*-1}4s¹ configuration by O₂ was interpreted by an attractive interaction correlated to a stable intermediate. The singly occupied antibonding π^* orbitals of O₂ are favorable to interact with singly occupied 3d orbitals of Co or Ni to form the intermediate. The depletion of the ground states of both atoms by NO indicated the occurrence of efficient termolecular processes at the low-pressure condition and implied the formation of a long-lived intermediate by the interaction between the 4s orbital and the singly occupied π orbital.

Introduction

Information about the gas-phase kinetics for reactions of simple molecules with transition-metal atoms provides fundamental information about catalytic bond activation. Their nearly degenerate *ns* and (*n*-1)*d* orbitals provide a unique opportunity to study the roles of their electronic configuration and electronic energy on reactions, because there are several electronic states with different electron configurations within a narrow energy range. In spite of the importance from both basic and application points of view, little is known about reactions of gas-phase transition-metal atoms compared with transition-metal cations.¹

Recently, a laser-induced fluorescence technique was used combined with a dc-discharge²⁻¹¹ or laser photolytic formation of gas-phase transition-metal atoms,¹²⁻¹⁶ and these studies provide useful information on the bimolecular reactions of the transition-metal atoms. In some cases, such information is extended to the interaction of electronically excited states as well as the ground state.⁶⁻¹³ These studies have shown that ground states, 3d^{*n*-2}4s² configuration in most cases, are inert, while the excited states of the 3d^{*n*-1}4s¹ configuration are very active with most reactants. Since the 3d^{*n*-1}4s¹ configuration correlates to higher electronic energies in Ti and V, it is difficult to discriminate the effect of the electron configuration from the effect of the electronic energy. Therefore, two explanations have been proposed in the case of reactions of Ti and V with oxidants. One is the electron-transfer mechanism where the electronic energy is a more dominant factor. In the reactions with molecules of positive electron affinities, the electron-transfer mechanism can explain the relative reaction rates of Ti(a^3F), V(a^4F), Ti(a^5F), and V(a^6D) semiquantitatively.⁶⁻⁸ The other explanation is the orbital correlation between the reactant and the product, metal oxide. In this mechanism, the electron configuration is a more dominant factor. Recent studies of the reactions of Mo(a^7S_3 , a^5S_2 , a^5D_J , a^5G_J) with O₂ have shown that the a^7S_3 and a^5S_2 states (4d⁵5s¹ configuration) were more

reactive than the a^5D state (4d⁴5s² configuration), although the a^5D state has a higher electronic energy.¹² Unfortunately, little is known about the potential energy surfaces for the interaction of the transition-metal atoms with simple molecules, and these interpretations are speculative. We believe that more experimental information, even though phenomenological, is required for a wide variety of reaction systems.

In this work, we have studied the reactions of neutral cobalt and nickel atoms in their ground electronic states and in their first and second excited states, Co(a^4F , b^4F , and a^2F) and Ni(a^3F , a^3D , and a^1D), with oxygen-containing molecules. The electron configurations and energies of these states are summarized in Table 1.¹⁷ These energies are also shown in Figure 1 with energy levels of early transition metals, Ti and V. As can be seen in Figure 1, these systems provide the following unique conditions for studying the details of the interaction between transition-metal atoms and simple molecules:

(1) Strong spin-orbit coupling in Co or Ni provides large splittings among spin-orbit sublevels. In the depletions of early transition-metal atoms, i.e., Sc, Ti, or V, rate constants have been observed to be independent of the spin-orbit levels.¹⁸ This has been interpreted partly by very fast interconversion among these levels upon collision with buffer gases. The large spin-orbit splitting in cobalt and nickel could provide a unique condition to study the effect of spin-orbit levels on the interaction of these atoms with small molecules.

(2) The same electron configuration forms different spin states which have similar energies. This condition provides the opportunity to study the effect of spin multiplicity and surface crossings.

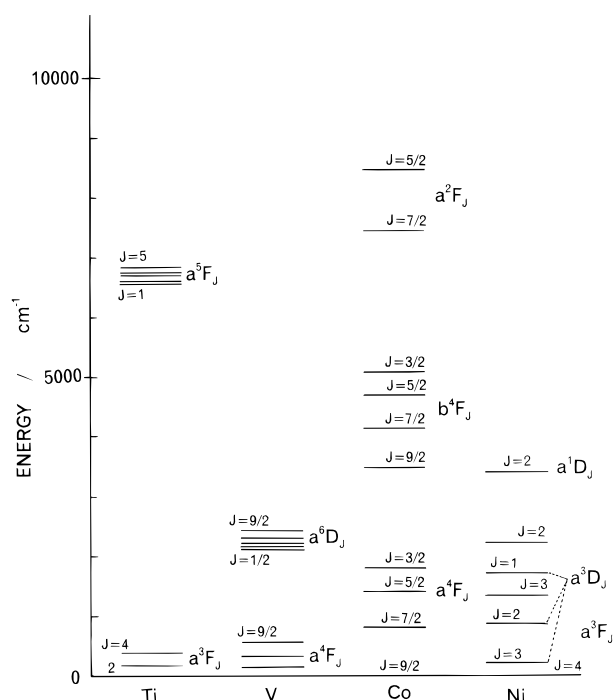
(3) A unique property in Ni is that two triplet states are lying in the same energy region. Although the collisional interconversion between these states could be very fast because of the small energy difference, it is possible to study the effect of the electron configuration on the interaction with oxygen-containing molecules under the same energy conditions.

These late transition-metal atoms have more than half-filled 3d orbitals, and metal oxide formation is energetically inacces-

[⊗] Abstract published in *Advance ACS Abstracts*, December 15, 1996.

TABLE 1: Configurations and Energies of the Low-Lying States of Co and Ni^a

atom	configuration	term	<i>J</i>	energy, cm ⁻¹
Co	3d ⁷ 4s ²	a ⁴ F	9/2	0.00
			7/2	816.00
			5/2	1406.84
			3/2	1809.33
			1/2	1809.33
	3d ⁸ 4s ¹	b ⁴ F	9/2	3482.82
			7/2	4142.66
			5/2	4690.18
			3/2	5075.83
			1/2	5075.83
3d ⁸ 4s ¹	a ² F	7/2	7442.41	
		5/2	8460.81	
		3/2	8460.81	
		1/2	8460.81	
		1/2	8460.81	
Ni	3d ⁸ 4s ²	a ³ F	4	0.000
			3	1332.153
			2	2216.519
			1	2216.519
			1	2216.519
	3d ⁹ 4s ¹	a ³ D	3	204.786
			2	879.813
			1	1713.080
			1	1713.080
			1	1713.080
3d ⁹ 4s ¹	a ¹ D	2	3409.925	
		1	3409.925	
		1	3409.925	
		1	3409.925	
		1	3409.925	

^a Data taken from ref 17.**Figure 1.** Electronic energy level diagram of the low-lying states of Ti, V, Co, and Ni.

sible for their ground states in the interaction with O₂ and NO. Even though the electronic energy is taken into account, only electronic energy transfer is possible for O₂ and NO as a bimolecular process. Therefore, these systems provide the opportunity to study the entrance channel interaction.

Experimental Section

A flow tube/LIF instrument used in these experiments has been described in detail previously.⁶ Briefly, metal atoms were created in a dc-discharge source where a cobalt (Nilaco, 99.99%) or nickel (Nilaco, 99.99%) rod was used as the cathode. The atoms are carried downstream in the He buffer gas (300 K). About 5% Ar was added to the flow to stabilize the discharge, and the reactant gas was introduced 24 cm downstream from the metal source. The densities of the unreacted metal atoms were measured by laser-induced fluorescence (LIF) at known atomic transitions. He (99.9999%), Ar (99.9999%), O₂ (99.9999%), NO (99.9%), and N₂O (99%) gases were obtained from NIHON SANSO and used without further purification. A capacitance

TABLE 2: LIF Transitions Used To Probe Co(a⁴F, b⁴F, and a²F) and Ni(a³F, a³D, and a¹D)^a

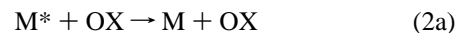
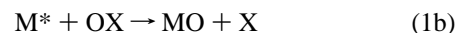
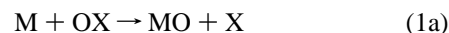
species	transition	energy, cm ⁻¹	wavelength, nm
Co(a ⁴ F)	<i>z</i> ⁶ G _{11/2} –a ⁴ F _{9/2}	25 568.68	391.10
	<i>z</i> ⁴ F _{9/2} –a ⁴ F _{7/2}	27 529.86	363.24
	<i>z</i> ⁴ F _{7/2} –a ⁴ F _{5/2}	27 370.43	365.36
	<i>z</i> ⁴ F _{5/2} –a ⁴ F _{3/2}	27 407.04	364.87
	<i>z</i> ⁴ F _{3/2} –a ⁴ F _{1/2}	27 370.43	365.36
Co(b ⁴ F)	<i>z</i> ⁴ G _{9/2} –b ⁴ F _{9/2}	25 786.91	387.79
	<i>z</i> ⁴ D _{7/2} –b ⁴ F _{9/2}	25 811.70	387.42
	<i>z</i> ⁴ D _{5/2} –b ⁴ F _{7/2}	25 806.10	387.51
	<i>z</i> ⁴ D _{3/2} –b ⁴ F _{5/2}	25 753.45	388.30
	<i>z</i> ⁴ D _{1/2} –b ⁴ F _{3/2}	25 666.82	389.61
Co(a ² F)	<i>y</i> ² G _{7/2} –a ² F _{7/2}	26 691.18	374.66
	<i>y</i> ² G _{7/2} –a ² F _{5/2}	25 672.78	389.52
Ni(a ³ F)	<i>z</i> ⁵ F ₄ –a ³ F ₄	29 084.478	343.83
	<i>z</i> ⁵ F ₂ –a ³ F ₃	28 830.987	346.85
	<i>z</i> ³ D ₁ –a ³ F ₂	28 696.319	348.48
	<i>z</i> ¹ F ₃ –a ³ F ₂	28 814.523	347.05
Ni(a ³ D)	<i>z</i> ⁵ F ₄ –a ³ D ₃	28 879.692	346.26
	<i>z</i> ³ F ₃ –a ³ D ₂	28 440.969	351.61
	<i>z</i> ³ F ₂ –a ³ D ₁	28 906.360	345.94
	<i>z</i> ³ D ₁ –a ³ D ₁	29 199.758	342.47
Ni(a ¹ D ₂)	<i>z</i> ⁵ F ₃ –a ¹ D ₂	29 832.810	378.46

^a Energies and wavelengths are derived from data in ref 17.

manometer (MKS Baratron, Type 122A) was used to measure the total pressure inside the flow tube, and thermal mass flowmeters (KOFAC Model 3710) were used to measure the flow rates of the reactant gas and He.

A tunable titanium sapphire laser (Continuum TS-60) or a tunable dye laser (Continuum ND-60) with LDS698 dye were used to measure the density of the cobalt or nickel atoms. Both lasers were pumped by a Nd:YAG laser (Continuum NY-82). To obtain the wavelength for the transitions of the cobalt and nickel atoms, the frequencies of these tunable lasers were doubled by a KD*P crystal and a bandpass filter was used to eliminate fundamental radiation. The transitions and energies used for detecting the electronic states of Co and Ni are summarized in Table 2. For some states whose populations and the LIF signal levels are low, two different transitions were used to confirm the measurements. Spectrally unresolved fluorescence was collected by a lens system and focused through a 2.0-mm slit into a photomultiplier tube (PMT) (HAMAMATSU Photonics R-928). The PMT current was amplified by a wide-band preamplifier (NF Electronics, Model BX-31) and the amplified voltage pulse was integrated by a boxcar integrator (SRS, Model SR-250).

Rate Constant Determination. In the systems studied here, the following processes are possible, where M* and OX[‡] indicate an excited state of metal atom and vibrational excited OX, and X = O, N, N₂:

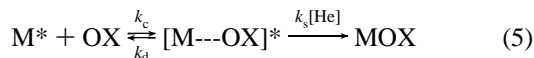


Among the three oxidants used here, the simple bimolecular reactions, eqs 1a and 1b, are energetically possible only for N₂O. The quenching processes, eqs 2a and 2b, are accessible only for the electronically excited states. The time-integrated rate expressions for the simple bimolecular processes, eqs 1 and 2, are given by

$$\ln[M(n_{\text{OX}})/M_0] = -(k_{\text{rxn}} + k_{\text{q}})t_{\text{rxn}}n_{\text{OX}} \quad (4)$$

$M(n_{\text{OX}})$ is the time-integrated metal atom concentration, M_0 is the metal atom concentration when no reactant gas is present, t_{rxn} is the mean reaction time, n_{OX} is the reactant number density, and k_{rxn} and k_{q} are the rate constants of the bimolecular reaction and quenching, respectively.

All electronic states could be depleted via termolecular associations, eqs 3a and 3b. The termolecular association reaction, eqs 3a and 3b, can be given by the following mechanism:



$[\text{M}---\text{OX}]^*$ formed at the total collision rate constant (k_{c}) may be stabilized by collision with He (at k_{s}) or unimolecularly dissociate back to reactants (at k_{d}). Phenomenologically, the depletion rate constant, k_{phen} , is given by

$$k_{\text{phen}} = k_{\text{c}}k_{\text{d}}[\text{He}]/(k_{\text{s}} + k_{\text{d}}[\text{He}]) \quad (6)$$

Under constant He pressure, the time-integrated rate expression including processes 1–3 is given by

$$\ln[M(n_{\text{OX}})/M_0] = -(k_{\text{rxn}} + k_{\text{q}} + k_{\text{phen}})t_{\text{rxn}}n_{\text{OX}} \quad (7)$$

Laser-induced fluorescence intensities with reactant concentration n_{OX} and without reactant gas, $I(n_{\text{OX}})$ and I_0 , are proportional to $M(n_{\text{OX}})$ and M_0 , respectively. Therefore, the rate constants, $k_{\text{rxn}} + k_{\text{q}} + k_{\text{phen}}$, were derived by fitting semilogarithmic plots of $I(n_{\text{OX}})/I_0$ vs n_{OX} using a least-squares routine. We refer to these values as effective rate constants. The reaction time, t_{rxn} , was determined by laser vaporization–chemiluminescence measurement.⁶ Under 0.7 and 1.2 Torr of He pressure conditions, they were 2.0 and 1.3 ms, respectively.

One possible error of the depletion rate constants may come from fluorescence quenching. Collisions of reactants during lifetimes of the excited states of the LIF transition quench the fluorescence and cause phenomenological depletion of metal atoms. It is possible to estimate the collision frequencies during the lifetimes. The maximum partial pressures of the reactants are typically 0.01 Torr. By using hard-sphere rate constants, k_{HS} ,¹⁹ the collision rate is around $1 \times 10^5 \text{ s}^{-1}$. The fluorescence rates of the excited states are 1×10^7 to $1 \times 10^8 \text{ s}^{-1}$.²⁰ Since they are 2–3 orders of magnitude larger than the collision frequencies, we conclude that the fluorescence quenching is negligible for our experimental conditions.

We report two standard deviations as the uncertainty for the precision of the fits to multiple data sets. The accuracies are limited mainly by the atom production source. Other smaller contributions to our absolute uncertainty are from the measurement of t_{rxn} , incomplete mixing of the reagent gases, and the accuracy of the flow rate and pressure measurements. We estimate the absolute sensitivity of our instrument to be $\sim 5 \times 10^{-14} \text{ cm}^3 \text{ s}^{-1}$ based on our ability to easily observe a 5% decrease in our signal at a reagent gas flow rate of 100 sccm.

Results

The effective rate constants determined in this study are summarized in Tables 3–5. The depletions of the ground state of Co and low-lying triplet states of Ni were inefficient for all oxidants studied here. No large difference was observed between the rate constants of the two triplet states of Ni which have different electron configurations. The two excited states of Co and the singlet excited state of Ni were very reactive.

TABLE 3: Effective Bimolecular Rate Constants for the Reactions of Co(a^4F , b^4F , a^2F) and Ni(a^3F , a^3D , a^1D) with O_2

reaction	k_{expl} , $10^{-12} \text{ cm}^3 \text{ s}^{-1}$		E_{max} , ^b kJ/mol
	(0.7 Torr of He)	$k_{\text{HS}}^a/k_{\text{expl}}$	
Co($a^4F_{9/2}$) + O_2	NR	> 3900	20.6
Co($a^4F_{7/2}$) + O_2	NR		
Co($a^4F_{5/2}$) + O_2	NR		
Co($a^4F_{3/2}$) + O_2	NR		
Co($b^4F_{9/2}$) + O_2	33 ± 3	6.0	4.5
Co($b^4F_{7/2}$) + O_2	57 ± 12	3.5	3.1
Co($b^4F_{5/2}$) + O_2	103 ± 26	1.9	1.6
Co($b^4F_{3/2}$) + O_2	115 ± 24	1.7	1.3
Co($a^2F_{7/2}$) + O_2	75 ± 20	2.6	2.4
Co($a^2F_{5/2}$) + O_2	52 ± 24	3.8	3.3
Ni(a^3F_4) + O_2	NR	> 3900	20.6
Ni(a^3F_3) + O_2	0.1 ± 0.02	1900	18.8
Ni(a^3F_2) + O_2	0.6 ± 0.1	320	14.4
Ni(a^3D_3) + O_2	NR	> 3900	20.6
Ni(a^3D_2) + O_2	NR	> 3900	20.6
Ni(a^3D_1) + O_2	0.30 ± 0.06	640	16.1
Ni(a^1D_2) + O_2	186 ± 64	1.0	0.1

^a k_{HS} 's are hard-sphere rate constants calculated by using the diameters of the metal atoms and molecules and averaged relative velocities (see ref 19). ^b $E_{\text{max}} = -RT \ln(k_{\text{expl}}/k_{\text{HS}})$.

TABLE 4: Effective Bimolecular Rate Constants for the Reactions of Co(a^4F , b^4F , a^2F) and Ni(a^3F , a^3D , a^1D) with NO

reaction	k_{expl} , $10^{-12} \text{ cm}^3 \text{ s}^{-1}$		$k_{\text{HS}}^a/k_{\text{expl}}^b$	E_{max} , ^c kJ/mol
	0.7 Torr of He	1.2 Torr of He		
Co($a^4F_{9/2}$) + NO	1.4 ± 0.3	2.2 ± 0.4	146	12.4
Co($a^4F_{7/2}$) + NO	1.7 ± 0.4	2.2 ± 0.5	120	11.9
Co($a^4F_{5/2}$) + NO	1.9 ± 0.4	2.7 ± 0.5	110	11.7
Co($a^4F_{3/2}$) + NO	2.0 ± 0.4		100	11.5
Co($b^4F_{9/2}$) + NO	77 ± 16		2.6	2.4
Co($b^4F_{7/2}$) + NO	93 ± 19		2.2	2.0
Co($b^4F_{5/2}$) + NO	93 ± 19		2.2	2.0
Co($b^4F_{3/2}$) + NO	110 ± 22		1.9	1.6
Co($a^2F_{7/2}$) + NO	99 ± 20		2.1	1.9
Co($a^2F_{5/2}$) + NO	90 ± 18		2.3	2.1
Ni(a^3F_4) + NO	2.1 ± 0.4	3.4 ± 0.7	94	11.3
Ni(a^3F_3) + NO	4.9 ± 1.0		40	9.2
Ni(a^3F_2) + NO	3.9 ± 0.8		51	9.8
Ni(a^3D_3) + NO	2.1 ± 0.4	2.5 ± 0.5	94	11.3
Ni(a^3D_2) + NO	2.1 ± 0.4	2.8 ± 0.6	94	11.3
Ni(a^3D_1) + NO	3.6 ± 0.7	4.6 ± 0.9	55	10.0
Ni(a^1D_2) + NO	5.5 ± 1.1		36	8.9

^a k_{HS} 's are hard-sphere rate constants calculated by using the diameters of the metal atoms and molecules and averaged relative velocities (see ref 19). ^b k_{expl} 's of 0.7 Torr of He are used. ^c $E_{\text{max}} = -RT \ln(k_{\text{expl}}/k_{\text{HS}})$.

One interesting point mentioned in the Introduction is the difference among spin–orbit sublevels. It is clear from Tables 3–5 that the rate constants of the spin–orbit sublevels belonging to the same electronic state were different in some systems. Among the four levels of Co(b^4F), the rate constants increase with the energy; i.e., Co($b^4F_{9/2}$) has the smallest rate constant and Co($b^4F_{3/2}$) has the largest one. Some sublevels of Ni(a^3F , a^3D) show depletion upon the interaction with O_2 or N_2O ; however, the other sublevels do not. Such a difference in rate constants among the same electronic state was not observed in the cases of Ti and V with oxidants; i.e., the rate constants for the spin–orbit sublevels were identical to one another.^{6,8} These have been interpreted to mean that the interconversion among the spin–orbit levels is very fast upon the collision with buffer gas.⁶ However, this is not the case for Co and Ni. Co and Ni have large energy spacings between the spin–orbit levels. That is, the energy differences between the highest level and the lowest level in Co(b^4F) and Co(a^2F) are 1593 and 1018 cm^{-1} , respectively. These are much larger than those of Ti(a^3F) (387

TABLE 5: Effective Bimolecular Rate Constants for the Reactions of Co(a^4F , b^4F , a^2F) and Ni(a^3F , a^3D , a^1D) with N_2O

reaction	$k_{\text{expl}}, 10^{-12} \text{ cm}^3 \text{ s}^{-1}$ (0.7 Torr of He)	$k_{\text{HS}}^a/k_{\text{expl}}$	$E_{\text{max}}^b, \text{ kJ/mol}$
Co($a^4F_{9/2}$) + N_2O	NR	>4100	20.7
Co($a^4F_{7/2}$) + N_2O	NR	>4100	20.7
Co($a^4F_{5/2}$) + N_2O	0.50 ± 0.22	410	15.0
Co($a^4F_{3/2}$) + N_2O	0.44 ± 0.09	460	15.3
Co($b^4F_{9/2}$) + N_2O	33 ± 9	6.2	4.5
Co($b^4F_{7/2}$) + N_2O	32 ± 14	6.3	4.6
Co($b^4F_{5/2}$) + N_2O	35 ± 9	5.8	4.4
Co($b^4F_{3/2}$) + N_2O	25 ± 6	8.1	5.2
Co($a^2F_{7/2}$) + N_2O	24 ± 6	8.5	5.3
Co($a^2F_{5/2}$) + N_2O	37 ± 12	5.5	4.3
Ni(a^3F_4) + N_2O	NR	>4000	20.7
Ni(a^3F_3) + N_2O	5.9 ± 1.2	34	8.8
Ni(a^3F_2) + N_2O	14 ± 3	14	6.6
Ni(a^3D_3) + N_2O	NR	>4000	20.7
Ni(a^3D_2) + N_2O	NR	>4000	20.7
Ni(a^3D_1) + N_2O	10 ± 2	20	7.4
Ni(a^1D_2) + N_2O	14 ± 3	14	6.6

^a k_{HS} 's are hard-sphere rate constants calculated by using the diameters of the metal atoms and molecules are averaged relative velocities (see ref 19). ^b $E_{\text{max}} = -RT \ln(k_{\text{expl}}/k_{\text{HS}})$.

cm^{-1}) and Ti(a^5F) (286 cm^{-1}), which are comparable to the thermal energy, 210 cm^{-1} .²¹ Therefore, the interconversion among the spin-orbit levels by collisions with He is expected to be much slower for Co and Ni, possibly allowing for a difference in rate constants to be observed. The difference in rate constants among the spin-orbit levels has been also observed in the oxidation of Mo(a^5D_j)²² and Fe(a^5D_j),²³ where the energy differences between the highest level and the lowest one are larger than the thermal energy, i.e., 1481 and 978 cm^{-1} in Mo and Fe, respectively.

Co, Ni + O₂. The rate constants for the interaction of Co or Ni with O₂ are summarized in Table 3. No depletion was observed for the ground state of Co, Co(a^4F_j), whereas the first and second excited states of Co(b^4F_j , a^2F_j) showed very efficient depletion upon interaction with O₂. We also measured the rate constants at a higher He pressure, 1.2 Torr. The rate constants at the two pressures have no systematic differences and agree within experimental error, although there may be a contribution from termolecular reactions because the change of total pressure is small.

Figure 2 shows the normalized LIF intensity for Ni(a^3F_2) as a function of O₂ flow. Among six spin-orbit sublevels of the lowest two triplet states, only the upper three levels, Ni($a^3F_{2,3}$, a^3D_1), showed depletion and no depletion was observed for the lower three levels, Ni(a^3F_4 , $a^3D_{3,2}$). The rate constants were on the order of $10^{-13} \text{ cm}^3 \text{ s}^{-1}$ and the depletion was quite inefficient. Here, the rate constants depend on the spin-orbit sublevels, which is reasonable since in most combinations of the two sublevels, the spacings are larger than the thermal energy. The only exception could be the spacing between Ni(a^3F_4) and Ni(a^3D_3), i.e., 204.79 cm^{-1} . Compared with the triplet states, Ni(a^1D_2) showed very efficient depletion. Figure 3 shows the normalized LIF intensity of Ni(a^1D_2) as a function of the O₂ flow, which has a measured rate constant of $(186 \pm 64) \times 10^{-12} \text{ cm}^3 \text{ s}^{-1}$.

Co, Ni + NO. The rate constants for the interaction of Co or Ni with NO are summarized in Table 4. Unlike O₂, all the states studied here including Co(a^4F_j) and Ni(a^3F_4 , $a^3D_{3,2}$) showed depletion upon interaction with NO. Because the ground spin-orbit levels of Co and Ni, Co($a^4F_{9/2}$) and Ni(a^3F_4), have only termolecular process, eqs 3a, we measured the rate constants for these levels at two different He pressures, 0.7 and

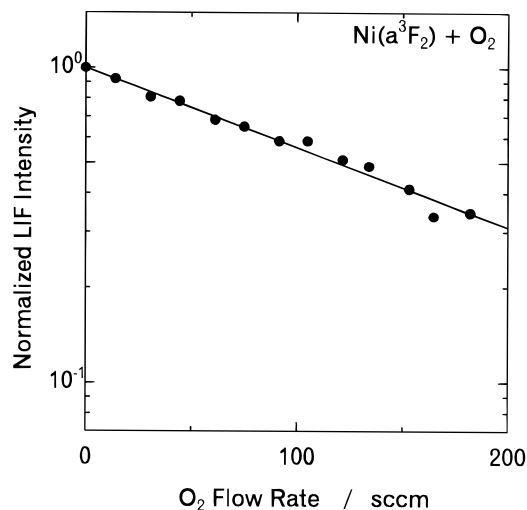


Figure 2. Semilogarithmic plots of the $M(n_{\text{OX}})/M_0$ LIF intensities for Ni(a^3F_2) vs flow of O₂. The solid line is the optimized least-squares fit of eq 7 to the data.

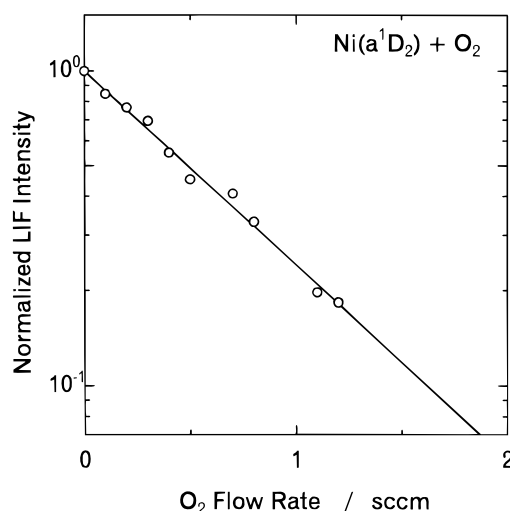


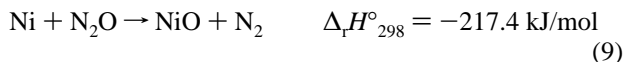
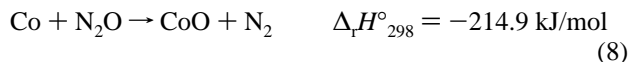
Figure 3. Semilogarithmic plots of the $M(n_{\text{OX}})/M_0$ LIF intensities for Ni(a^1D_2) vs flow of O₂. The solid line is the optimized least-squares fit of eq 7 to the data.

1.2 Torr. For comparison, the rate constants were also measured for some of the other levels in Co(a^4F_j) and Ni(a^3F_j , a^3D_j) at two He pressures. The results are also listed in Table 4. In the all systems, the higher He pressure provides a little larger rate constant, which implies that the depletion has a contribution from the termolecular process, reaction 5. According to eq 6, the second-order rate constant will increase with the He pressure at low pressure condition. Our data show systematic increase of the rate constants by the increase of the He pressure, though the increase may not be large enough to fit our data with eq 6. Since no bimolecular depletion channel is energetically possible for the lowest spin-orbit levels of Co and Ni, Co($a^4F_{9/2}$) and Ni(a^3F_4), the termolecular process, reaction 5, is only the explanation, which is consistent with the pressure-dependent rate constants for both states as observed. However, in the cases of the other sublevels, there may be some contribution from the bimolecular process.

Among the spin-orbit levels, the rate constants show no systematic difference larger than experimental errors. As mentioned above, the interconversion among the spin-orbit levels by collisions with the buffer gas are not fast enough to wash out the difference of rate constants. Therefore, similar rate constants among the levels indicate that the depletion efficiencies are similar for all sublevels.

The depletion of the singlet excited state of Ni by NO was not efficient in contrast with that of O₂. The rate constant was of the same order of magnitude as those of Ni(a^3F , a^3D). The two excited states of Co showed efficient depletion upon interaction with NO. The rate constants of the spin-orbit levels are different from one another in both electronic states. Co(a^2F) showed little smaller rate constants than Co(b^4F), and this result is similar to the depletion by O₂.

Co, Ni + N₂O. The rate constants for the interaction of Co or Ni with N₂O are summarized in Table 5. The following reactive channels are energetically possible for the interaction of Co or Ni with N₂O.²⁴



Although these reactions are energetically possible for all levels, the lowest energy spin-orbit levels, Co($a^4F_{9/2,7/2}$) and Ni(a^3F_4 , $a^3D_{3,2}$), show no depletion upon interaction with N₂O. Co($a^4F_{5/2,3/2}$) were depleted inefficiently, and Ni($a^3F_{2,3}$, a^3D_1) were depleted rather efficiently. We have measured the rate constants for Co($a^4F_{5/2,3/2}$) at two He pressures; however, no systematic difference was observed.

Ni(a^1D) was depleted at the same rate as the lower energy triplet states of Ni, Ni(a^3F_2 , a^3D_1). Among the four sublevels of Co(b^4F) and two sublevels of Co(a^2F), the rate constants were the same within experimental errors. Because the interconversion among these sublevels by collisions with the buffer gas is not fast enough to smear out the difference of the rate constants, these results indicate that the rate constants of these levels are the same.

Discussion

Product Channels. As mentioned in the Experimental Section, one possible process of depletion is the association reaction, reaction 5. Under the low-pressure condition, the rate constant of the association reaction is expected to show a pressure dependence (eq 6). Among the interactions of Co or Ni with the oxidants studied here, only Co(a^4F_j) + NO and Ni(a^3F_j , a^3D_j) + NO showed a little pressure dependence. Even in the other reactions, our pressure range may not be large enough to show a clear pressure dependence in the rate constants, and it is useful to consider the extent of the association reaction.

For the ground state of Co and Ni, the termolecular rate constants with O₂ under Ar buffer gas conditions have been determined at 298 K.²⁵ The termolecular process of Co + O₂ is very inefficient, and the rate constant is less than $(1.0 \pm 0.3) \times 10^{-32} \text{ cm}^6 \text{ s}^{-1}$. The ground state of Ni has a larger rate constant, $(1.7 \pm 0.3) \times 10^{-30} \text{ cm}^6 \text{ s}^{-1}$. If this rate constant for Ni is used to estimate the contribution from the termolecular reaction, the second-order rate constant at 0.7 Torr of Ar is calculated to be $0.04 \times 10^{-12} \text{ cm}^3 \text{ s}^{-1}$. This value is 1 order of magnitude smaller than the rate constants determined in this study for Ni($a^3F_{3,2}$, a^3D_1). The rate constant for Co may not be applied for the excited states, since the termolecular rates for the electronic states of the $3d^{n-1}4s^1$ configuration have been reported to be larger than those of the $3d^{n-2}4s^2$ configuration. One typical rate constant is given by the termolecular rate of Cr(a^7S , $3d^54s^1$); i.e., the rate constant of the termolecular association with O₂ by using Ar as the third body is $(6.5 \pm 1.1) \times 10^{-29} \text{ cm}^6 \text{ s}^{-1}$.²⁶ If this rate constant is used, the second-order rate constant with 0.7 Torr of He is expected to be $1.6 \times 10^{-12} \text{ cm}^3 \text{ s}^{-1}$. This value is 1–2 orders of magnitude smaller

than the rate constants determined for Co(b^4F_j , a^2F_j). Therefore, we concluded that most of the depletion in the interaction between Co or Ni and O₂ is due to a bimolecular process.

For the interaction of Co or Ni with NO or N₂O, no termolecular reaction has been measured. If we take the termolecular rate constant for Cr + NO or N₂O as a measure for the termolecular rate of the $4s^1$ state, the limiting second-order rate constants for removal of ground-state Cr by NO and N₂O are $(1.0 \pm 0.1) \times 10^{-14}$ and $3.0 \times 10^{-14} \text{ cm}^3 \text{ s}^{-1}$, respectively,²⁶ smaller than our detection limit. This is consistent with the results of Co + N₂O and Ni + N₂O. Although the termolecular process is possible for the lowest energy sublevels, they showed no depletion. If the rate constant of the termolecular process does not depend highly on the spin-orbit level within the same electronic state, the process is negligible for the Co + N₂O and the Ni + N₂O systems. On the other hand, the depletion rate constants for the Co + NO and the Ni + NO systems show a little pressure dependence. Although the dependence is small, this is consistent with the occurrence of the termolecular reaction which could be the only explanation of the depletion of the ground states, Co($a^4F_{9/2}$) and Ni(a^3F_4).

Among the bimolecular processes, eqs 1 and 2, the oxide formation is not accessible for NO and O₂. While the electronic-to-translational (E-T) energy transfer is possible for any excited state, the electronic-to-vibrational (E-V) energy transfer is only possible for Co(b^4F_j , a^2F_j) and Ni(a^1D_2). Although no direct experimental evidence is obtained, much larger rate constants for Co(b^4F_j , a^2F_j) and Ni(a^1D_2) with O₂ and NO could imply the occurrence of the E-V energy transfer. The reaction channels are only available for Co + N₂O and Ni + N₂O systems. Metal oxide formation, eqs 8 and 9, is accessible for the ground states of Co and Ni. The dissociation energy of O–N₂ is $167.1 \pm 0.5 \text{ kJ/mol}$ which corresponds to the formation of O(3P) + N₂. The ground state of N₂O is not directly correlated to this channel but to O(1D) + N₂. Even if we take into account the electronic energy, 1.967 eV, the oxide formation channels are energetically possible. Although no enhancement of Ni(a^3F_4 , a^3D_3 , a^3D_2) was observed, this may not indicate that the depletion is entirely via reaction 9, since the enhancement is proportional to the initial populations of the upper states which could be very small. In some experiments, a little enhancement of Co($a^4F_{5/2, 3/2}$) was observed on interaction with N₂O. Although it could be difficult to specify the initial states of the enhancement, this result implies that the electronic energy transfer can be important even in reactive systems like Co + N₂O.

Reaction Efficiencies and Activation Energies. One way to describe the efficiencies of the depletion processes measured in this study is to compare the measured rate constants with calculated hard-sphere rate constants, k_{HS} .¹⁹ These comparisons are given as $k_{\text{HS}}/k_{\text{expl}}$ values in Tables 3–5. These values indicate that Ni(a^3F , a^3D) needs more than a few hundred collisions for depletion by O₂, while only one to six collisions are enough to deplete Ni(a^1D) and Co(b^4F , a^2F). Assuming that these systems are governed by an Arrhenius behavior, $k(T) = Ae^{-E_{\text{max}}/RT}$, and the hard-sphere rate constants can be used as upper limits for the A factor, we can calculate the upper limits for the activation energy (E_{max}). These results are also listed in Tables 3–5. Very inefficient depletion of Ni(a^3F , a^3D) provides very high E_{max} 's, i.e., 14–19 kJ/mol. In the depletion of Ni(a^1D) and Co(b^4F , a^2F), the estimated E_{max} 's are less than 1 kcal/mol, which indicates that these depletion processes probably have no barrier or the barrier is very low if one exists.

In the cases of Co + NO and Ni + NO, the depletion

efficiencies for Co(a^4F) and Ni(a^3F , a^3D) are around 100 collisions for depletion. The estimated E_{\max} 's are around 10 kJ/mol. Ni(a^1D) needs about 40 collisions to be depleted by NO, and E_{\max} is 9 kJ/mol. This inefficiency is different from the interaction with O₂ where almost every collision leads to depletion of Ni(a^1D). Only the excited states of Co(b^4F , a^2F) show about the same order of rate constants as the gas kinetic collision and the E_{\max} 's are a few kilojoules/mole.

Reaction Mechanisms. Co, Ni + O₂. In order to have some insight into the reaction mechanism, it is useful to compare the rate constants determined here with those of the other transition-metal systems. Ti(a^5F) + N₂ and V(a^6D) + N₂ are used, since no reactive channel is accessible. The reported rate constants are $(6.5 \pm 2.2) \times 10^{-12}$ and $(0.50 \pm 0.03) \times 10^{-12}$ cm³ s⁻¹, respectively, and have been explained by the crossing between two repulsive surfaces.⁶ The ground states and the first excited states of Ti and V have electron configurations of 3d²4s²(3d³-4s²) and 3d³4s¹(3d⁴4s¹), respectively. Due to the large spatial extent of the closed 4s subshell, the surface evolving from the ground state is expected to be repulsive at longer Ti or V + N₂ distances than those evolving from the first excited state, where the 4s orbital is only singly occupied. As the Ti or V and N₂ distance decreases, surfaces evolving from the ground state and the first excited state cross. With spin-orbit interaction that effectively moves one electron from a 3d orbital and places it into the 4s orbital, the electronic energy transfer is accomplished. The difference between Ti and V has been ascribed to the electronic-to-vibrational energy transfer which is only possible for the Ti + N₂ system.

The rate constants for Co(b^4F , a^2F) + O₂ and Ni(a^1D) + O₂ are much larger than for Ti(a^5F) + N₂, while those of Ni(a^3F , a^3D) + O₂ are the same order of magnitude as those of V(a^6D) + N₂. The latter may be reasonable because the vibrational energy of O₂, 1580 cm⁻¹, is only accessible for Ni(a^3F_2) + O₂($v=0$) → Ni(a^3D_3) + O₂($v=1$),²⁷ and most sublevels can be depleted by electronic-to-translational energy transfer which is same as for V(a^6D) + N₂. One difference could be the contribution of an attractive potential for the Ni + O₂ system. *Ab initio* calculation has predicted the presence of the complex NiO₂, which is stable by 75 kJ/mol with respect to the Ni(a^3D) + O₂ asymptote.²⁸ According to the calculation, this complex has a 4s¹ configuration and the spin state is singlet. Since one of the potential surfaces from Ni(a^3D) + O₂($X^3\Sigma$) could be correlated to this complex, an attractive well could be formed. However, the rate constants determined here are small, and the estimated maximum activation energies, E_{\max} 's, are rather high, and they are suggesting no attractive well.

On the other hand, the rate constants for Co(b^4F , a^2F) and Ni(a^1D) are much larger than that for Ti(a^5F) + N₂. In both systems, the E-V energy transfer is possible. The high efficiencies of the depletion processes by O₂ imply the occurrence of a favorable entrance channel interaction between Co(b^4F , a^2F) or Ni(a^1D) and O₂. One possible mechanism to make the potential attractive could be the interaction between a singly occupied 3d orbital and a singly occupied π^* antibonding orbital of O₂. If we assume C_{2v} geometry where the Co or Ni atom approaches along the z axis and the O-O axis is parallel to x, the 3d_{yz} orbital has the same symmetry as the $p\pi_z^*$ orbital of O₂, both orbitals are singly occupied and could interact attractively. An intermediate formed via this interaction is expected to have an elongated O-O bond because there is more population in the $p\pi_z^*$ orbital. Therefore, the formation of such an intermediate is also favorable to form vibrationally excited O₂ as the product. This mechanism can be applied to both Co and Ni, although there are a different number of electrons. Since

Ni has one more electron, the interaction between $p\pi_z^*$ and 3d_{yz} suggests the configuration of the intermediate has singly occupied 4s and $p\pi_y^*$ orbitals. If the reaction starts from Ni(a^1D) + O₂($^3\Sigma_g^-$), these two electrons must be in the triplet state. However, *ab initio* calculation has predicted that the lowest state of the triangular NiO₂ is a singlet state as mentioned above.²⁸ When we take into account the inefficiency of the process which proceeds on the singlet surface evolved from Ni(a^3D) + O₂($^3\Sigma_g^-$), our results suggest that the triplet surface of NiO₂ is more stable than the singlet one.

The intermediate complex formation is also useful to explain the relative order of rate constants. Among the four levels in Co(b^4F_1), the higher energy levels show larger rate constants. In the complex mechanism, the number of exit channels depends on the energy content in the complex. Therefore, the intermediate formed from the higher levels can access more exit channels if the formation of the intermediate does not depend on the spin-orbit levels.

Co, Ni + NO. One difference in the depletion by NO vs that by O₂ is detectable depletion of the states with 4s² configuration, Co(a^4F) and Ni(a^3F). Although the depletion processes were ascribed to the termolecular association reaction, the rate constants observed here require the adduct formed by the bimolecular collision, [M-NO][‡], lives long enough to be stabilized by collisions with He.²⁹ This implies the presence of an attractive interaction between NO and the transition-metal atom of the 4s² state. Among the three oxidants studied here, NO is reported to deplete early transition-metal atoms, Sc, Ti, and V, most efficiently despite its low electron affinity.^{3,8} The activation energies for Ti(a^3F) + NO and V(a^4F) + NO are much smaller than those for Ti(a^3F) + O₂ and V(a^4F) + O₂³⁰ and imply that the interaction of NO with the metal atoms of the 4s² configuration are more attractive than those of O₂. One favorable property of NO could be the presence of the singly occupied π orbital which is localized on the N atom. The interaction between this π orbital and 4s orbital could form an attractive interaction. Such an interaction is not possible in the case of O₂, since the singly occupied π^* orbital has a counterpart with opposite phase at the second O atom, which would cause additional repulsion.

The effective depletion of the 3d⁸4s¹ states of Co could be ascribed to the attractive interaction between the singly occupied 3d orbital of Co and the π orbital of NO, as similar to the case of Co + O₂. The only difference from the case of Co or Ni + O₂ is the stable geometry. That is, C_{2v} geometry has no advantage in the case of Co + NO, and linear one, Co-N-O, is favorable for the overlap between one of the 3d orbitals and the singly occupied π orbital.

Co, Ni + N₂O. The depletion of Co and Ni by N₂O is similar to that by O₂. The lowest energy spin-orbit levels show no depletion, and the depletion becomes efficient with increasing electronic energy. This is reasonable for the depletion by O₂, because only the electronic energy transfer is available as the bimolecular process. However, the reactive channels, eqs 8 and 9, are energetically possible for all spin-orbit levels in the interaction with N₂O, and our results indicate the presence of energy barriers in the reaction channels. An interesting difference between N₂O and O₂ is that the depletion by N₂O depends on the electronic energy and there seems to be a common threshold energy for both metal atoms. In Figure 4, the rate constants are plotted as a function of the electronic energy for three systems. In the interaction with O₂, Ni(a^3F , a^3D) shows the threshold behavior; however, no depletion was observed for even Co($a^4F_{3/2,5/2}$), which have higher energy than Ni(a^3F_3 , a^3D_1). However, Figure 4c indicates that the rate constants of

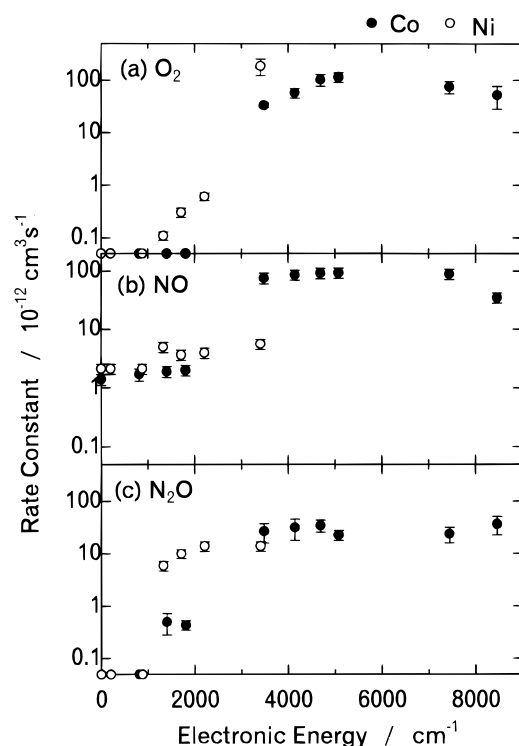


Figure 4. Semilogarithmic plots of the measured rate constants vs electronic energies.

both atoms start to rise at around 1000 cm^{-1} (12 kJ/mol). Although it may not be necessary that the onsets for both metals agree, these results indicate that the amount of electronic energy may be more important than the electron configuration.

The estimated E_{max} 's are listed in Table 5. The E_{max} 's for the lower reactive levels, Co($a^4F_{5/2,3/2}$) and Ni($a^3F_{3,2}$, a^3D_1), are 6.6–15.3 kJ/mol. If the electronic energies are added to these values, the activation energies measured from the ground spin-orbit levels are given as 24.7–36.9 kJ/mol. Reactions of a wide variety of metal atoms, including some transition-metal atoms, with N_2O have been studied. The activation energies of these reactions have been modeled by a resonance interaction model advanced by Fontijn and co-workers.^{31–34} In this model, the activation barriers are calculated by taking into account the ionization potential and sp promotion energy of the metal, the electron affinity of N_2O , and the bond energy of the metal oxide product. This model describes the reactions of many main group metals reasonably well. According to this model, the activation energies for Co and Ni with N_2O are estimated to be 31.5 and 32.7 kJ/mol, respectively.³¹ They are of the same order as our values estimated from the ground level. Although our E_{max} 's are only rough measures of the activation barriers, the agreement may be reasonable. The resonance interaction model has a limitation to predict the kinetic behavior of transition-metal atoms because it neglects both the d electrons of the transition metals and the product metal oxide's electronic structure. Recent measurements of the activation energies for the reactions of transition-metal atoms have shown discrepancies between the measured values and the predicted ones.¹⁶ Therefore, the measurement of temperature dependence of rate constants is highly required to obtain the activation energies.

The electronic energy transfer is also possible for these systems, and the activation energy of the energy transfer must be different from those from the resonance interaction model. The linear triatomic molecule N_2O has low-frequency vibrational modes, i.e., 589 and 1285 cm^{-1} for bending and NO stretching modes, respectively.³⁵ These low-frequency vibrational modes are useful for a E-V energy transfers.

Summary

The kinetics of depletion of Co and Ni upon interactions with O_2 , NO, and N_2O were studied in a fast-flow reactor at a He pressure of 0.70 Torr. The depletion rate constants were determined for the ground and the first and second excited states of both atoms, Co(a^4F_j , b^4F_j , a^2F_j) and Ni(a^3F_j , a^3D_j , a^1D_j). For all oxidants, quite inefficient or no depletion was observed for the ground states of both atoms. The low-lying excited state of Ni(a^3D_j) ($3d^94s^1$ configuration) also showed inefficient depletion, and no difference was observed between this state and the ground state, Ni(a^3F_j) ($3d^84s^2$ configuration). The first and second excited states of Co(b^4F_j , a^2F_j) ($3d^84s^1$ configuration) were depleted very efficiently by all oxidants. The depletion of Ni(a^3D_j) ($3d^94s^1$ configuration) depended on the oxidants; i.e., O_2 depleted this state by the gas kinetics rate constant, while the depletions by NO and N_2O were about 1 order of magnitude slower. Efficient depletion was interpreted by attractive interactions caused by stable intermediates. The metal atoms of $3d^{n-1}4s^1$ configuration could form intermediates with O_2 or NO by the interactions between the 3d orbitals of Co or Ni and the singly occupied π^* orbital of O_2 or the π orbital. The depletion of the ground states of both atoms by NO indicated the occurrence of efficient termolecular processes at the low-pressure condition and could imply the attractive interaction between the singly occupied π orbital and the filled 4s orbital.

Acknowledgment. This work is supported partly by grants (Grant-in-Aid for Scientific Research on Priority Areas, Free Radical Science, and Chemistry of Small Manybody System) from the Japanese Ministry of Education, Science, and Culture.

References and Notes

- (1) For example, see: Armentrout, P. B.; Beauchamp, J. L. *Acc. Chem. Res.* **1989**, *22*, 315.
- (2) Ritter, D.; Carroll, J. J.; Weisshaar, J. C. *J. Phys. Chem.* **1992**, *96*, 10636.
- (3) Ritter, D.; Weisshaar, J. C. *J. Phys. Chem.* **1990**, *94*, 4907, 1576.
- (4) Ritter, D.; Weisshaar, J. C. *J. Am. Chem. Soc.* **1990**, *112*, 6425.
- (5) Ritter, D.; Weisshaar, J. C. *J. Phys. Chem.* **1989**, *93*, 1576.
- (6) Clemmer, D. E.; Honma, K.; Koyano, I. *J. Phys. Chem.* **1993**, *97*, 11480.
- (7) Honma, K.; Nakamura, M.; Clemmer, D. E.; Koyano, I. *J. Phys. Chem.* **1994**, *98*, 13286.
- (8) Honma, K.; Clemmer, D. E. *Laser Chem.* **1995**, *15*, 209.
- (9) Honma, K. *J. Chinese Chem. Soc.* **1995**, *42*, 371.
- (10) Senba, K.; Matsui, R.; Honma, K. *J. Phys. Chem.* **1995**, *99*, 13992.
- (11) Matsui, R.; Senba, K.; Honma, K. *Chem. Phys. Lett.* **1996**, *250*, 560.
- (12) Campbell, M. L.; McClean, R. E.; Harter, J. S. *Chem. Phys. Lett.* **1995**, *235*, 497.
- (13) McClean, R. E.; Pasternack, L. *J. Phys. Chem.* **1992**, *96*, 9828.
- (14) Campbell, M. L.; McClean, R. E. *J. Phys. Chem.* **1993**, *97*, 7942.
- (15) McClean, R. E.; Campbell, M. L.; Goodwin, R. H. *J. Phys. Chem.* **1996**, *100*, 7502.
- (16) Campbell, M. L. *J. Chem. Phys.* **1996**, *104*, 7515.
- (17) Sugar, J.; Corliss, C. *J. Phys. Chem. Ref. Data* **1985**, *14*, Suppl. No. 2.
- (18) A small dependence on the spin-orbit levels has been reported in the depletion of Mo(a^3D_j) + O_2 in ref 12.
- (19) The hard-sphere rate constants are calculated by $k_{HS} = \pi/4(d_M + d_{OX})^2 \langle v \rangle$. The diameters of O_2 , NO, and N_2O are 3.43, 3.47, and 3.88 Å as given in: Hirschfelder, J. O.; Curtiss, C. F.; Bird, R. B. *Molecular Theory of Gases and Liquids*; Wiley: New York, 1954; Table I-A. The diameters of Co and Ni are taken to be 3.34 and 3.24 Å, and all electronic states are assumed to have the same diameter. The mean relative velocity, $(8k_B T / \pi \mu)^{1/2}$, was used for $\langle v \rangle$ where k_B , T , and μ were the Boltzmann's constant, temperature, and reduced mass, respectively.
- (20) Fuhr, J. R.; Martin, G. A.; Wiese, W. L. *J. Phys. Chem. Ref. Data* **1988**, *17*, Suppl. No. 4.
- (21) Same is true for V, i.e., 552.96 and 313 cm^{-1} for a^4F and a^6D , respectively. All energies of the spin-orbit levels were taken from ref 17.
- (22) McClean, R. E.; Campbell, M. L.; Goodwin, R. H. *J. Phys. Chem.* **1996**, *100*, 7502.
- (23) Campbell, M. L.; Metzger, J. R. *Chem. Phys. Lett.* **1996**, *253*, 158.

(24) $D^{\circ}_{298}(\text{N}_2\text{-O})=167.1 \pm 0.5$ kJ/mol is derived from values of $\Delta_i H^{\circ}_{298}$ given in: Chase, M. W.; Davies, C. A.; Downey, J. R.; Frurip, D. J.; McDonald, R. A.; Syverud, A. N. *J. Phys. Chem. Ref. Data* **1985**, *14*, Suppl. 1 (JANAF tables). $D^{\circ}_{298}(\text{Co-O}) = 384 \pm 13$ kJ/mol and $D^{\circ}_{298}(\text{Ni-O}) = 381 \pm 17$ kJ/mol are from: Pedley, J. B.; Marshall, E. M. *J. Phys. Chem. Ref. Data* **1983**, *12*, 967.

(25) Brown, C. E.; Mitchell, S. A.; Hacket, P. A. *J. Phys. Chem.* **1991**, *95*, 1062.

(26) Parnis, J. M.; Mitchell, S. A.; Hacket, P. A. *J. Phys. Chem.* **1990**, *94*, 8152.

(27) Although $\text{Ni}(\text{a}^3\text{D}_1) + \text{O}_2(\nu=0) \rightarrow \text{Ni}(\text{a}^3\text{F}_4) + \text{O}_2(\nu=1)$ is also energetically possible the $\Delta J = 3$ transition could be inefficient.

(28) Blomberg, M. R. A.; Siegbahn, P. E. M.; Strich, A. *Chem. Phys.* **1985**, *97*, 287.

(29) Under our flow conditions, the mean time during collisions with He is estimated to be 1.5×10^{-7} s.

(30) The activation energies for $\text{Ti}(\text{a}^3\text{F}) + \text{NO}$ and $\text{V}(\text{a}^4\text{F}) + \text{NO}$ are 3.62 ± 0.71 and 1.67 ± 0.79 kJ/mol, respectively, while those for $\text{Ti}(\text{a}^3\text{F}) + \text{O}_2$ and $\text{V}(\text{a}^4\text{F}) + \text{O}_2$ are 11.6 ± 0.8 and 9.04 ± 0.79 kJ/mol, respectively (ref 14).

(31) Futerko, P. M.; Fontijn, A. *J. Chem. Phys.* **1991**, *95*, 8065.

(32) Futerko, P. M.; Fontijn, A. *J. Chem. Phys.* **1992**, *97*, 3861.

(33) Futerko, P. M.; Fontijn, A. *J. Chem. Phys.* **1993**, *98*, 7004.

(34) Belyung, D. P.; Futerko, P. M.; Fontijn, A. *J. Chem. Phys.* **1995**, *102*, 155.

(35) Shimanouchi, T. *Tables Molec. Vibrational Freq., NSRDS-NBS*, **1972**, 39.